Journal of Solid State Chemistry 182 (2009) 502–508

Contents lists available at ScienceDirect

Journal of Solid State Chemistry

journal homepage: www.elsevier.com/locate/jssc

Synthesis, structural characterization and selectively catalytic properties of metal–organic frameworks with nano-sized channels: A modular design strategy

Ling-Guang Qiu [a,*], Li-Na Gu [a], Gang Hu [a], Li-De Zhang [b]

[a] School of Chemistry and Chemical Engineering, Anhui University, 3rd, Feixi Road, Hefei 230039, PR China
[b] Institute of Solid State Physics, Chinese Academy of Sciences, Hefei 230031, China

ARTICLE INFO

Article history:
Received 17 August 2008
Received in revised form
9 November 2008
Accepted 19 November 2008
Available online 27 November 2008

Keywords:
Modular design
Metal–organic framework
Heterogeneous catalysis
Microporous materials
Host–guest systems

ABSTRACT

Modular design method for designing and synthesizing microporous metal–organic frameworks (MOFs) with selective catalytical activity was described. MOFs with both nano-sized channels and potential catalytic activities could be obtained through self-assembly of a framework unit and a catalyst unit. By selecting hexaaquo metal complexes and the ligand BTC (BTC = 1,3,5-benzenetricarboxylate) as framework-building blocks and using the metal complex $[M(phen)_2(H_2O)_2]^{2+}$ (phen = 1,10-phenanthroline) as a catalyst unit, a series of supramolecular MOFs 1–7 with three-dimensional nano-sized channels, i.e. $[M^1(H_2O)_6]\cdot[M^2(phen)_2(H_2O)_2]_2\cdot 2(BTC)\cdot xH_2O$ (M^1, M^2 = Co(II), Ni(II), Cu(II), Zn(II), or Mn(II), phen = 1,10-phenanthroline, BTC = 1,3,5-benzenetricarboxylate, $x = 22-24$), were synthesized through self-assembly, and their structures were characterized by IR, elemental analysis, and single-crystal X-ray diffraction. These supramolecular microporous MOFs showed significant size and shape selectivity in the catalyzed oxidation of phenols, which is due to catalytic reactions taking place in the channels of the framework. Design strategy, synthesis, and self-assembly mechanism for the construction of these porous MOFs were discussed.

1. Introduction

Microporous metal–organic frameworks (MOFs) are crystalline materials assembled by the bonding of metal ions with polyfunctional organic ligands. Their attributes include high porosity, spatial and chemical tailoring, and synthetic scalability [1–3]. They have attracted great attention of chemists, material scientists, and physical scientists since 1990s due to interest in the creation of nano-sized spaces and their potential application in gas storage [4], adsorption and separation [5], catalysis [6–15], molecular sensing [16], photonics [17,18] as well as magnetic materials [19]. Compared with traditional porous carbons, inorganic zeolites and recently developed MCM (mobile crystalline material)-type mesoporous materials, microporous MOFs are synthesized under mild conditions and hold great promise for their ease of processability, flexibility, structural diversity, and geometrical control. As a result, numerous microporous MOFs with various structures and different physicochemical properties have been reported.

MOFs with nano-sized channels offer great potential for the direct incorporation of catalytic sites. It could be expected that MOFs containing uniformly sized and shaped pores could open possibilities for size- and shape-selectivity effects. Consequently, selective heterogeneous catalysis of organic transformations has been expected to be one of the most important and the most promising applications of microporous MOFs ever since 1990s [1–3,6]. However, compared with the rapid developments and numerous studies on their applications in selective adsorption, molecular exchange and separation, especially the latest howling successes in hydrogen storage [20–22], only a handful of successful examples in designing and synthesizing microporous MOFs with heterogeneous catalytic activities can be found in the literature [6–15]. The inherent reason for this limitation can be attributed to the fact that most microporous MOFs contain no coordinatively unsaturated metal center (UMC). To date, it is still a challenge for scientists to rationally design and construct microporous MOFs for selective catalytic reactions.

When designing and constructing porous MOFs with potential catalytic activity, the key challenge is not only to introduce UMCs into the framework but also to create void spaces for selective catalysis. For the design of microporous MOFs, however, transition metal ions or metal complexes with potential catalytic activities are selected as building blocks to construct the framework rather

* Corresponding author. Fax: +86 551 5107342.
E-mail address: lgqiu@ahu.edu.cn (L.-G. Qiu).

0022-4596/$ - see front matter © 2008 Elsevier Inc. All rights reserved.
doi:10.1016/j.jssc.2008.11.018

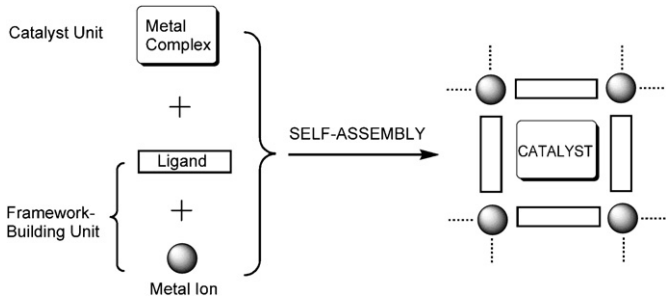

Scheme 1. Illustration of the modular design strategy.

than for the design of MOF-type catalysts containing catalytically active sites. In general, the metal ions have a tendency to coordinate to organic ligands, thus leading to the loss of the UMCs in the framework in most cases. In order to obtain porous MOFs with potential catalytic activities, scientists have to design and synthesize various multifunctional organic ligands with specific structures and various topologies [10–12]. Recently, we have demonstrated that supramolecular MOFs with three-dimensional (3-D) nano-sized channels, in which transition metal complexes are encapsulated, possess significant size- and shape-selective catalytic activities for oxidation of phenols [8]. In the present work, we present a concept for the construction of microporous MOFs with potential heterogeneous catalytic activities, i.e. "modular design" strategy (Scheme 1). According to this method, the microporous MOF with potential catalytic activity can be assembled in a simple manner by two building modules: (a) the framework module, which is constructed by an organic ligand and transition metal ions and (b) the functional module (i.e. catalyst unit in this work). Self-assembly of these two building modules under a proper condition will result in MOFs with both pores and the catalyst in the framework. It should be noted that the concept of modular design strategy described here is quite different from modular self-assembly reported previously [23,24]. In the case of the latter, modular self-assembly relies upon two molecular components that are not individually capable of self-assembly and can be invoked to construct coordination polymers or multiple-component hydrogen-bonded frameworks. By selecting the framework-building blocks and the catalyst unit, a series of supramolecular microporous MOFs (**1**–**7**), $[M^1(H_2O)_6(BTC)_2]\cdot[M^2(phen)_2(H_2O)_2]_2\cdot xH_2O$ (BTC = 1,3,5-benzenetricarboxylate; phen = 1,10-phenanthroline; M^1, M^2 = Co(II), Ni(II), Cu(II), Zn(II), or Mn(II), $x = 22$–24), were designed and synthesized using modular design strategy. Catalytic activities of these MOFs were tested by catalyzed oxidation of phenols, and these compounds showed significant size-selective catalysis for the oxidation of phenol and 1-naphthol. Remarkably, these porous MOFs possess unique shape-selective activity for the oxidation of phenol. Based on the experimental results, design strategy and self-assembly mechanism for the construction of these supramolecular microporous MOFs were discussed. The preliminary results suggest that the modular design strategy is a convenient approach to the design and the construction of microporous MOFs with selective catalytic activities.

2. Experimental and methods

2.1. Instruments

Infrared (IR) spectra (KBr pellets) were recorded in the 400–4000 cm^{-1} range using a Nocolet Nexus 870 FTIR spectrometer. Thermal gravimetric analysis (TGA) was performed under N_2 atmosphere with a heating rate of 5 °C using a Perkin-Elmer Pyris 1 TGA system. The elemental analyses of C, H, N were carried out on a Perkin-Elmer 2400 elemental analyzer, and metal contents were determined by Leeman PLA-SPEC ICP. Powder X-ray diffraction (XRD) data were recorded on a Philips-1700X diffractometer (Cu-$K\alpha$ radiation, $\lambda = 0.154178$ nm). The products of oxidation of phenols were analyzed by gas chromatograph Varian 3800 equipped with a CP-8 column and a flame ionization detector.

2.2. Syntheses of 1–7

Identical synthetic procedures were used to prepare the compounds **1–7**, those of the homonuclear compound **2** and heteronuclear compound **6** were described here in detail. An aqueous solution of Na_3BTC and a mixture solution of $ZnCl_2$ and *cis*-$[Zn(phen)_2]Cl_2$ were allowed to diffuse slowly in a U-shaped tube, across an agar gel medium at 2 ± 0.05 °C, to yield cubic-shaped crystals of $[(Zn(phen)_2(H_2O)_2)_2(Zn(H_2O)_6)(BTC)_2]\cdot22H_2O$ within 4 weeks. When $NiCl_2\cdot6H_2O$ was used instead of $ZnCl_2$, a heteronuclear 3-D framework $[(Zn(phen)_2(H_2O)_2)_2(Ni(H_2O)_6)(BTC)_2]\cdot22H_2O$ (**6**) formed. All the compounds were characterized by elemental analysis and IR. Structures of compounds **1–6** were also characterized using single-crystal XRD method. Although single-crystal of **7** of high quality suitable for single-crystal X-ray analysis was not obtained in this work, both elemental analysis and IR results as well as XRD pattern of compound **7** reveal that compounds **1–7** are isostructural (Fig. S1, see supporting information). Elemental analysis calcd (%) for **1**: C 41.41, H 5.54, N 5.86; found: C 41.76, H 5.41, N 6.02; IR (KBr, cm^{-1}): 1618(s), 1558(s), 1427(s), 1365(s), 1101(m), 850(m), 775(m). Elemental analysis calcd (%) for **2**: C 41.55, H 5.39, N 5.88; found: C 41.48, H 5.27, N 5.94; IR (KBr, cm^{-1}): 1618(s), 1565(s), 1429(s), 1378(s), 771(m). Elemental analysis calcd (%) for **3**: C 41.99, H 5.45, N 5.94; found: C 42.02, H 5.41, N 6.09; IR (KBr, cm^{-1}): 1612(s), 1556(s), 1430(s), 1363(s), 775(m), 723(s). Elemental analysis calcd (%) for **4**: C 41.97, H 5.44, N 5.94; found: C 41.92, H 5.32, N 6.11; IR (KBr, cm^{-1}): 1614(s), 1560(s), 1427(s), 1363(s), 771(m), 725(m). Elemental analysis calcd (%) for **5**: C 42.02, H 5.41, N 5.94, Cu 3.37, Mn 5.83; found: C 42.26, H 5.23, N 6.13, Cu 3.52, Mn 6.31; IR (KBr, cm^{-1}): 1616(s), 1560(s), 1429(s), 1363(s), 848(m), 773(m), 725(s). Elemental analysis calcd (%) for **6**: C 41.70, H 5.41, N 5.90, Ni 3.09, Zn 6.88; found: C 41.98, H 5.21, N 6.15, Ni 3.14, Zn 6.94; IR (KBr, cm^{-1}): 1618(s), 1558(s), 1427(s), 1365(s), 850(m), 775(m), 725(s). Elemental analysis calcd (%) for **7**: C 41.67, H 5.40, N 5.89, Cu 10.02; found: C 41.81, H 5.34, N 5.96, Cu 10.38; IR (KBr, cm^{-1}): 1612(s), 1554(s), 1426(s), 1360(s), 852(m), 723(s). All compounds show similar IR spectra due to the fact that they are isostructural. A strong absorbance at ~1615 cm^{-1} indicates the presence of a carbon–oxygen double bond and can be designated as the symmetrical stretch of COO^-. The absorption band at ~1560 cm^{-1} can be designated as the asymmetrical stretch of COO^-, and the absence of an adsorption band at ~1700 cm^{-1} reveals that all carboxylic groups of the ligand H_3BTC in the MOFs obtained are deprotonated. In addition, the presence of absorption bands at ~725 cm^{-1} indicates the formation of Cu–O coordination bonds in these compounds.

2.3. Single-crystal X-ray structure determination

Crystallographic measurements were carried out on a Siemens SMART CCD diffractometer with graphite-monochromated Mo-$K\alpha$ radiation ($\lambda = 0.071073$ nm) at 298 K. The structures were solved by direct methods using SHELXS-97 [25,26] and were refined by full-matrix least-squares methods using SHELXL-97 [27] on F^2.

Non-hydrogen atoms were refined anisortropically except for disordered atoms. Hydrogen atoms on carbon atoms were generated geometrically and refined isotropically.

Crystal data for **2**: $C_{33}H_{51}N_4O_{22}Zn_{1.5}$, $M_r = 953.83$, crystal size $= 0.42 \times 0.35 \times 0.21$ mm, monoclinic, space group $P2_1/c$, $a = 1.2763(6)$, $b = 1.8980(10)$, $c = 1.8067(9)$ Å, $\beta = 90.000\ (8)^\circ$, $V = 4377(4)$ Å^3, $Z = 4$, $\rho_{calcd} = 1.448$ g cm^{-3}, $\mu = 0.913$ mm^{-1}; of 22 548 measured reflections ($\theta = 1.56$–25.04), 7744 were independent. $R_1 = 0.0487$ [$I > 2\sigma(I)$], w$R_2 = 0.0823$. **3**: $C_{66}H_{102}N_8O_{44}Ni_3$, $M_r = 1887.69$, crystal size $= 0.28 \times 0.21 \times 0.18$ mm, $a = 1.2695(9)$, $b = 1.8943(13)$, $c = 1.8063(12)$ Å, $\beta = 90.110\ (12)^\circ$, $V = 4344(5)$ Å^3, $Z = 2$, $\rho_{calcd} = 1.443$ g cm^{-3}, $\mu = 0.742$ mm^{-1}; of 22 598 measured reflections ($\theta = 1.56$–25.03), 7673 were independent. $R_1 = 0.0585$ [$I > 2\sigma(I)$], w$R_2 = 0.1191$. **4**: $C_{66}H_{102}Co_3N_8O_{44}$, $M_r = 1888.35$, crystal size $= 0.32 \times 0.19 \times 0.16$ mm, $a = 1.2695(6)$, $b = 1.8985(9)$, $c = 1.8018(8)$ Å, $\beta = 90.140\ (7)^\circ$, $V = 4343(3)$ Å^3, $Z = 2$, $\rho_{calcd} = 1.444$ g cm^{-3}, $\mu = 0.665$ mm^{-1}; of 22 694 measured reflections ($\theta = 1.56$–25.03), 7671 were independent. $R_1 = 0.0518$ [$I > 2\sigma(I)$], w$R_2 = 0.1334$. **6**: $C_{66}H_{102}N_8NiO_{44}Zn_2$, $M_r = 1901.01$, crystal size $= 0.31 \times 0.24 \times 0.16$ mm, $a = 1.2609(7)$, $b = 1.8866(9)$, $c = 1.7962(9)$ Å, $\beta = 90.000\ (10)^\circ$, $V = 273(4)$ Å^3, $Z = 2$, $\rho_{calcd} = 1.478$ g cm^{-3}, $\mu = 0.875$ mm^{-1}; of 21 575 measured reflections ($\theta = 1.57$–25.03), 7539 were independent. $R_1 = 0.0696$ [$I > 2\sigma(I)$], w$R_2 = 0.1705$. $R_1 = (\Sigma||F_0 - F_c||/\Sigma|F_0|)$; $R_w = \{\Sigma w(F_0 - F_c)^2/\Sigma w(F_0)^2\}^{1/2}$.

2.4. Catalytic measurements

Catalytic experiments to test catalytic activities of compounds **1–7** were carried out in a 50 ml glass reaction flask fitted with a water condenser. Crystals of the catalyst were ground in a mortar until they became microcrystalline powder. Typically, phenols (0.06 mol), ethanol (10 ml), and the powder of the catalyst (20 mg) were added to the flask, respectively. The mixture solution was heated to 35 °C with mechanically stirring at 800 rpm, then a solution of H_2O_2 (30 wt%, 4.53 g, 0.04 mol) in ethanol (10 ml) was added dropwise over a period of about 2 h. The reaction was continued for another 7 h at 35 °C. The products were analyzed using a gas chromatograph.

3. Results

3.1. Structural description

Compounds **1–7** have a common formula $[M^1(H_2O)_6]\cdot[M^2(phen)_2(H_2O)_2]_2(BTC)_2\cdot xH_2O$ (M^1, M^2 = Co(II), Ni(II), Cu(II), Zn(II), or Mn(II); $x = 22-24$). Generally speaking, this kind of supramolecular assembly is constructed by a framework module, i.e. a two-dimensional (2-D) hydrogen-bonded host framework $[M(H_2O)_6(BTC)_2]^{4-}$ as well as a catalyst unit encapsulated in one-dimensional (1-D) channels created in the host framework (Figs. 1 and 2), i.e. metal complex $[M(phen)_2(H_2O)_2]^{2+}$. The single-crystal X-ray structural analysis of compounds **1–6** reveals that this type of supramolecular MOF consists of two cationic units $[M(phen)_2(H_2O)_2]^{2+}$ and $[M(H_2O)_6]^{2+}$, one anionic unit BTC, and guest water molecules in the asymmetric unit. Two kinds of six-coordinate metal centers can be found in the asymmetric unit, of which one metal center is coordinated to four nitrogen atoms from two chelating phenanthroline ligands and two oxygen atoms from water molecules, and the other one is coordinated to six oxygen atoms from water molecules (Fig. 3). Each BTC bridges two hexaaquo metal complex $[M(H_2O)_6]^{2+}$ by hydrogen bonds between the carboxylate oxygen atoms from BTC and coordinated water molecules from hexaaqua metal complex to form a 2-D

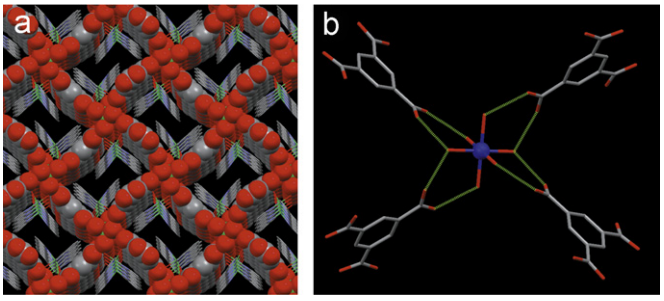

Fig. 1. (a) Molecular packing diagram of **1–6** along *a*-axis: the framework unit $[M(H_2O)_6(BTC)_2]$ is represented in space-filling style, showing 1-D channels running in this direction; the catalyst unit $[M(phen)_2(H_2O)_2]^{2+}$ encapsulated in the channels is represented in capped sticks format for clarity. All water guests have been omitted. Green: metal atom, red: O, and gray: C. (b) View of hydrogen-bonded building paddle-wheel SBU to construct the 2-D hydrogen-bonded host framework for **1–6** (blue: metal atom, red: O, gray: C, and green: hydrogen bonds formed between the carboxylate oxygen atoms from BTC and coordinated water molecules from the hexaaquo metal complex).

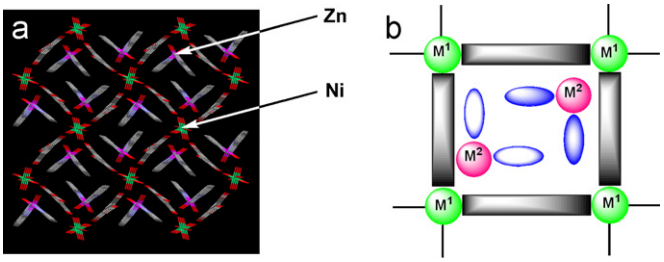

Fig. 2. (a) Molecular packing diagram along *a*-axis for heteronuclear complex **6** with Ni atoms in the framework unit and Zn atoms in the catalyst unit. (b) Illustration of heteronuclear metal–organic frameworks, showing metal atom M^1 in the framework.

hydrogen-bonded undulated layers stacked on each other (Fig. 4). Each undulated layer consists of two pair of shared edges rectangle with one $[M(H_2O)_6]^{2+}$ cation and one BTC anion at each corner and side, respectively. The rectangular channel has the dimension of approximately 16.7 × 12.3 Å for compound **1** and 16.5 × 12.2 Å for others (Fig. 1a), and the distance between the adjacent undulated layers is approximately 7.9–8.0 Å (Fig. 4). To the best of our knowledge, this is the first hydrogen bonded paddle-wheel secondary building unit (SBU) constructed by the hexaaquo metal complex and the aromatic polycarboxylate ligands (Fig. 1b). Moreover, although the catalyst unit (i.e. metal complex $[M(phen)_2(H_2O)_2]^{2+}$) occupies some of the channels created in the structure, space remains for solvent channels; the framework encapsulates a 3-D system of intersecting water-filled channels propagating along [001], [110] and [$\bar{1}$10]. After removing the guest water molecules, the void volumes in a unit cell are estimated as 1346–1361 Å^3 (ca. 30.5–30.7%) for frameworks **1–6**, respectively [27]. Although single crystal of compound **7** suitable for single crystal X-ray analysis was not obtained in the present work, IR, XRD patterns, and elemental analysis of **7** reveal that compounds **1–7** are isostructural (Fig. S1, see supporting information).

3.2. Thermal stability

In order to evaluate thermal stability of the frameworks **1–7**, TGA and XRD measurements at different temperatures were carried out. The results reveal that these supramolecular microporous MOFs are thermally stable until the coordinated water molecules evolve from the structures (see Figs. S2–S5). TGA on a crystalline sample for compound **1** (Fig. S6), for example, shows

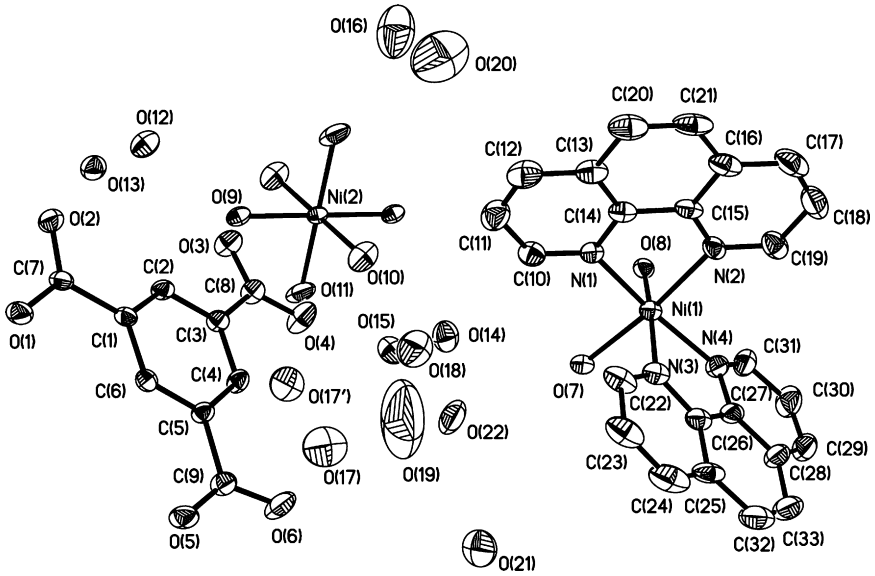

Fig. 3. Asymmetry unit of compound **3**; thermal ellipsoids are drawn at the 30% probably level; all hydrogen atoms are omitted for clarity.

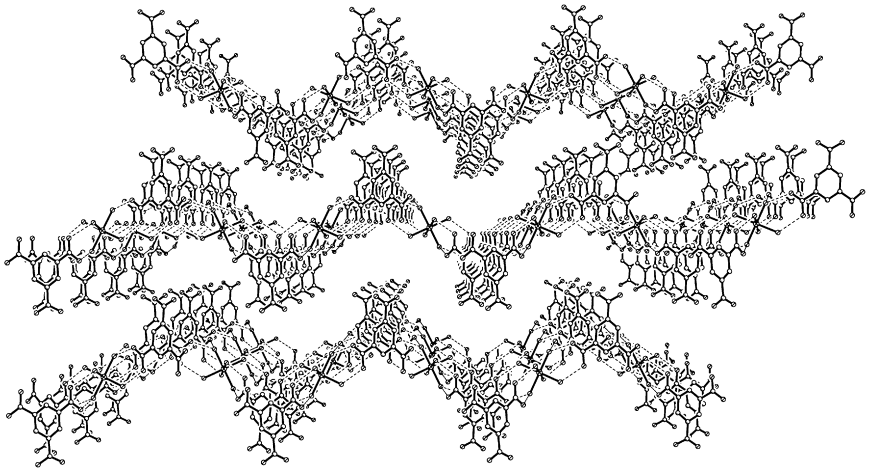

Fig. 4. Molecular packing diagram of complexes **1**–**6** along *c*-axis showing two-dimensional hydrogen-bonded undulated layers stacked on each other, metal complex $[M(phen)_2(H_2O)_2]^{2+}$, and all water guests are omitted for clarity.

the following clear and well-separated weight loss steps: a weight loss of 22.71% occurred over the temperature range 50–110 °C, corresponding to the loss of 22 water guests (calcd 22.59%), and a weight loss of 9.37% from 135 to 180 °C, corresponding to the loss of 10 coordinated water molecules per formula (calcd 9.41%). There is no weight loss during 180–460 °C. From 460–515 °C, there is the total loss of 55.01% consistent with the removal of phenanthroline and BTC molecules. The remaining weight of 12.91% corresponds to the percent (13.64%) of the Mn and O components, indicating that the final product is MnO_2.

3.3. Selective catalysis of phenols

Catalytic activities of **1**–**7** were tested by oxidation of phenol and 1-naphthol using H_2O_2 as oxidant. Oxidation of phenol or 1-naphthol using H_2O_2 in the absence of catalyst at 35 °C for 9 h only yields traces of products. Results of the oxidation of 1-naphthol catalyzed by compounds **1** and **5** at 35 °C for 9 h show only about 4% conversion of 1-naphthol. This conversion may be attributed to the catalytic reaction of oxidation occurring on the surface of the catalyst rather than in the channels of the framework, because molecular size of 1-naphthol is too large to diffuse into the channels of the framework. Remarkably, for the catalyzed oxidation of small-sized molecule phenol, which can

Table 1
Oxidation of phenol using H_2O_2 catalyzed by compounds **1**–**7**[a].

MOF	Framework unit	Catalyst unit	Conversion (wt%)
1	$[Mn(H_2O)_6(BTC)_2]$	$[Mn(phen)_2(H_2O)_2]$	21
2	$[Zn(H_2O)_6(BTC)_2]$	$[Zn(phen)_2(H_2O)_2]$	20
3	$[Ni(H_2O)_6(BTC)_2]$	$[Ni(phen)_2(H_2O)_2]$	17
4	$[Co(H_2O)_6(BTC)_2]$	$[Co(phen)_2(H_2O)_2]$	14
5	$[Cu(H_2O)_6(BTC)_2]$	$[Mn(phen)_2(H_2O)_2]$	21
6	$[Ni(H_2O)_6(BTC)_2]$	$[Zn(phen)_2(H_2O)_2]$	20
7	$[Cu(H_2O)_6(BTC)_2]$	$[Cu(phen)_2(H_2O)_2]$	16

[a] Phenol = 60 mmol; phenol/H_2O_2 = 1.5; catalyst = 20 mg; solvent = water/ethanol; reaction time = 9 h; reaction temperature = 35 °C.

freely diffuse in the channels formed in the framework, compounds **1**–**7** exhibit high catalytic activity; high phenol conversions (14–21%, see Table 1) are observed. This result reveals significant size-selectivity of this kind of microporous MOFs for the catalyzed oxidation of phenols.

Selective oxidation of phenol to hydroquinones is a very important organic transformation due to their important large-scale functions such as photographic film developer, antioxidant, polymerization inhibitor and medicines. Although many kinds of catalysts such as metal oxides, metal complexes, zeolites, or zeolite-encapsulated metal complexes have been developed for hydroxylation of phenol, in most cases, the ratio of hydroquinone/catechol (*para*/*ortho* ratio) is less than 1 [28], except for few excellent catalysts such as TS-1 [29]. However, for the catalyzed oxidation of phenol using compounds **1**–**8**, remarkably high *para*-selectivity (*para*/*ortho* ratio is 3.7 for compounds **1**–**6**, and 3.8 for compound **7**, respectively) is observed, although phenol conversion varies from 14% to 21%, respectively, which are lower than that using TS-1 [29]. This result reveals that this kind of supramolecular framework with nano-sized channels possesses significant shape-selective property, showing high *para*-selective activity for the catalyzed oxidation of phenol.

4. Discussion

4.1. Design strategy

Although numerous coordination polymers have been synthesized in the past few decades, most coordination polymers do not possess a porous structure. The tendency for framework interpenetration usually leads to a close packed structure, thus losing void space in the framework. As a result, the challenge to synthesize microporous MOFs for heterogeneous catalysis is not merely to introduce metal complexes into the framework. Furthermore, the coordinatively UMC in the catalyst unit may coordinate to the organic ligand that is intended for the construction of the framework, thus resulting in a coordinatively saturated metal center and losing potential catalytic activity. Consequently, in order to obtain MOFs with potential size- and/or shape-selectivities for heterogeneous catalysis, it is important to ensure both the valid space and the UMC in the framework.

We have ever selected a series of low-molecular-weight transition metal complexes with different structural characteristics as the catalyst unit, such as $M^{II}(SCN)_2$, $[M^{II}(en)_2]^{2+}$, and some metal complexes of microcyclic compounds (M = Cd, Zn, Ni, Co, Cu, and Mn, en = ethylenediamine), and used transition metal ions and 1,4-benzenedicarboxylate (BDC) or BTC as framework-building blocks, trying to assembled these low-molecular-weight metal complexes into the framework unit constructed by metal ions and BDC or BTC. By mixing aqueous solution of low-molecular-weight metal complex and metal ion with ligand BDC or BTC together, or letting BDC or BTC diffuse into the mixture solution of transition metal salt and the metal complex, the final product were obtained. Unfortunately, IR or single-crystals X-ray analysis of the resulting compounds revealed that the UMCs in the catalyst unit coordinated to the organic ligand selected as the framework-building block, leading to the loss of UMCs in the final assemblies. On the other hand, in some cases, ligand in the catalyst unit was completely substituted by the ligand BDC or BTC. This may be attributed to the fact that the carboxylate-type organic ligand BDC or BTC has a strong tendency to coordinate to transition metal ions. As a result, to successfully obtain porous MOFs that clathrate the catalyst unit using modular design strategy, some key obstacles should be overcome: (a) molecular recognition, orientation and fixation between catalyst unit and building blocks of the framework unit are necessary in the process of self-assembly, in order to prevent coordination reactions between framework-building blocks and UMCs in the catalyst unit; (b) framework interpenetration should be effectively avoided; and (c) sufficient void space remains even if the catalyst unit occupy part of the channels created in the framework.

Fortunately, supramolecular chemistry developed in recent years provides an effective means for scientists to design and generate organized equilibrium architectures with controllable structure and tunable properties. The final supramolecular entity evolves through a sequence of spontaneous but directed recognition, fixation, and assembly steps of suitably instructed components and specified interaction schemes. Non-covalent interactions, such as hydrogen bonding, π–π interactions, as well as electrostatic and hydrophobic forces, permit precise positioning of molecular components in a well-defined supramolecular architecture [30]. This approach offers the intriguing concept of inherent control over the dimensions and molecular recognition features that are present in porous structures. Consequently, modular design strategy may be realized using molecular recognition, fixation, and self-assembly of the catalyst unit and the framework-building unit as an effective tool through supramolecular interactions between two units.

4.1.1. Choosing of framework-building blocks

For modular design, in which the catalyst unit and framework unit should be assembled in a precisely controllable process, *N*-heterocycle aromatic ligands and aromatic carboxylate ligands, such as phenanthroline, bipyridine, BDC, or BTC, are excellent candidates. These aromatic ligands were selected because strong aromatic π–π stacking between the aromatic rings is always found in their assemblies, except for high thermal stability of their metal complexes; this aromatic π–π stacking effect is usually applied to design and construct supramolecular MOFs with controllable structures.

MOFs constructed by metal ions, phenanthroline (or bipyridine), and aromatic carboxylate ligands have been investigated extensively [31–39]. In general, their assemblies can be classified into two main categories: in the first case, both oxygen atom from carboxylate groups and nitrogen atoms from phenanthroline (or bipyridine) coordinate to the metal ions, resulting in a 1-D coordination polymeric chain or 2-D coordination sheet, by which a 3-D supramolecular framework may also be obtained through significant π–π interactions and hydrogen bonding [32–36]; in the second the metal atoms are chelated by phenanthroline or bipyridine, but no coordination reaction occurs between aromatic carboxylate and UMCs from metal complex of phenanthroline or bipyridine [32,33]. A typical example of such structure is $[Co(phen)_2(H_2O_2)_2](Ora)_2 \cdot 2.25H_2O$ (Ora = orotate), which is self-assembled from $[Co(HOra)(H_2O_2)_4] \cdot H_2O$ and phenanthroline at 60 °C [37]. The unique feature of this complex is that the cobalt atom is coordinated by a pair of bidentate phenanthroline molecules together with two water molecules, but the orotate anion does not coordinate to the cobalt atom. Furthermore, the mean plane through the orotate anion is almost parallel to that through the phenanthroline moiety due to significant aromatic stacking interaction. Obviously, it is orientation and fixation effects between phenanthroline and the carboxylate ligand through π–π interactions that blocks the coordination reaction between carboxylate ligand and UMC from metal complex $[Co(phen)_2]^{2+}$. For modular design, similarly, aromatic stacking interactions between the catalyst unit and the framework-building blocks could also be applied to design and construct microporous MOFs for selective catalysis through molecular

recognition, orientation, and fixation between the catalyst and the framework units.

4.1.2. Crystallization temperature

From previous studies [31–39] it could be found that crystallization temperature plays an important role in the construction of MOFs using transition metal ions, phenanthroline and aromatic carboxylate ligands as building blocks. For example, self-assembly of 1,2,4,5-benzenetetracarboxylate, phenanthroline, and transition metal ions at room temperature results in 2-D hydrogen-bonding frameworks being composed of one or more cationic unit, i.e. metal complex of phenanthroline, and an anionic unit, benzenetetracarboxylate [38,39]. However, hydrothermal or solvothermal reaction using the same building blocks leads to a 1-D coordination polymer, in which all the carboxylate groups of benzenetetracarboxylate coordinate to metal atom from metal complex of phenanthroline [35,36]. It is well known that bond energy of coordination linkage is much larger than those of hydrogen bond, electrostatic interaction, π–π interactions, or hydrophobic interaction. For entropic reasons, higher temperature is commonly advantageous for the formation of coordination bonds rather than hydrogen bonding and other supramolecular interactions. Consequently, synthesis at a higher temperature can promote the formation of polymeric frameworks of higher dimensionality through the loss of terminal ancillary ligands. Nevertheless, reaction at higher temperature would increase difficulties for people to utilize weaker supramolecular interactions such as hydrogen bonding and π–π interaction, although they have been demonstrated to be effective tools to design frameworks with more controllable structures. Especially for the modular design method, high temperature may lead to the formation of coordination bond between the UMC in the catalyst unit and the organic ligand used to construct the framework unit.

For the above reasons, in the present work, metal complexes of phenanthroline were selected as a catalyst unit, aromatic carboxylate ligand BDC or BTC and transition metal ions were selected as framework-building blocks, and the self-assembly was carried out at a low temperature to avoid the ligand binding to the UMC. Furthermore, in order to obtain frameworks with nanosized pores, it is naturally very important to avoid interpenetration of framework. Several methods have been developed to try to effect creation of space in the framework, for example varying the conditions of crystallization, templating using large guest molecules, and synthesizing extended ligand; among them template method has been demonstrated to be one of the most effective methods. For the modular design strategy in the present work, fortunately, the coordinatively UMC selected as the catalyst unit, could also be used as a template molecule, by which the framework interpenetration can be effectively avoided. Although template molecules occupy part of the channels in this case, space may remain for solvent channels.

4.2. Self-assembly mechanism

MOFs constructed by BTC, transition metal, and *N*-heterocycle such as phenanthroline and 2,2′-bipyridy have been systematically synthesized using hydrothermal method by Plater et al. [33], and the results reveal that the transition metal atoms are chelated by both *N*-heterocycle and carboxylate group from BTC, resulting in a 1-D polymeric chain. For modular design strategy, as mentioned above, high reaction temperature may lead to the loss of UMCs in the catalyst unit. Consequently, in contrast to hydrothermal reaction at 240 °C by Plater et al. [33], the crystallization temperature in the present work was selected as low as 2 °C. As expected, a kind of microporous supramolecular MOF

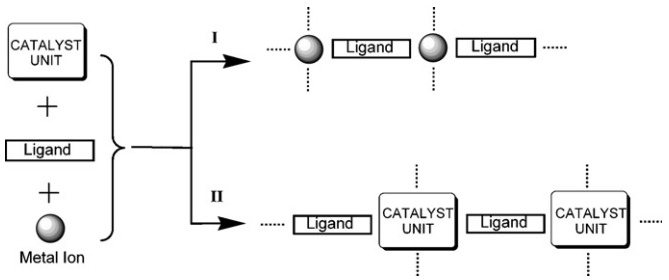

Scheme 2. Possibilities of assembly of catalyst unit, ligand, and metal ions at high reaction temperature.

with unique structure was obtained using BTC, transition metal ions, and metal complexes of phenanthroline as building blocks. Neither metal ions in hexaaquo metal complex nor the coordinatively unsaturated metal in the metal complexes of phenanthroline coordinate to carboxylate groups from BTC. Instead of coordination linkage, hydrogen bonds form between the oxygen atoms from carboxylic groups of BTC and the water molecules from the hexaaquo metal complex, forming a 2-D supramolecular framework. Also, a 1-D channel forms running along *a*-axis, in which the metal complex $[M(\text{phen})_2(H_2O)_2]^{2+}$ selected as both the catalyst unit and the template molecule is encapsulated. It should be noted that, although the catalyst unit occupies the 1-D channel created in the framework, around 30% of the volume is taken up by intersecting water-filled channels propagating along [001], [110] and [$\bar{1}$10] [8]. This could be attributed to large size of the template molecule (i.e. the catalyst unit, $[M(\text{phen})_2(H_2O)_2]^{2+}$) as mentioned above.

By comparing crystal structures obtained by low-temperature self-assembly in this work with those synthesized under hydrothermal conditions by Plater et al. [33], it is clear that varying assembly conditions, for example, synthesizing the MOFs at a low temperature or under hydrothermal condition, would lead to different assembly processes of framework-building blocks (i.e. metal ions and BTC) and catalyst unit. Lower temperature is advantageous for modular design method, while crystallization at high temperature leads to coordination linkage between the UMC in the catalyst unit and the ligand selected to construct the framework unit. For example, under hydrothermal conditions, the organic ligand used for the construction of framework may coordinate to metal ions, resulting in a coordination polymer, in which no catalyst unit is encapsulated (Type I, Scheme 2). On the other hand, the organic ligand may directly coordinate to the catalyst unit, thus leading to the loss of UMCs in the frameworks (Type II, Scheme 2). When the reaction is carried out at a low temperature, however, aromatic stacking interactions between phenanthroline and BTC ligands play an important role in the preorganization of the catalyst unit and framework-building blocks as well as in the self-assembly of compounds **1**–**7**. Consequently, a self-assembly process including continuous steps of molecular recognition, orientation, fixation, and assembly takes place (Scheme 1).

5. Conclusions

By using modular design method in a new way that involves the supramolecular self-assembly of a framework-building unit and a catalyst unit, a series of microporous supramolecular MOFs that contain catalytically active sites within the channels created in the framework were synthesized. Remarkable size- and shape-selective activities of these microporous MOFs were observed for the catalyzed oxidation of phenols due to catalytic reaction taking

place in the channels of the framework. The results suggest that the modular design strategy is a convenient approach to the design and the construction of microporous MOFs with coordinatively UMCs, and this design strategy described here provide new opportunities for size- and shape-selective catalyst. Also, by varying the framework-building blocks and tailor-made functional unit with different characteristics, modular design method can be applied to develop other kinds of functionalized MOFs, such as non-linear optical materials, sensors, and molecular magnetic materials, through self-assembly of the framework unit and the functional module.

Acknowledgments

This work was supported by the National Natural Science Foundation of China (20501001), the Key Research Project of Natural Science from Bureau of Anhui Province, China (kj2007A078), and the Selected Financial Support Research Project from Bureau of Anhui Province, China.

Supporting information

Supporting information containing TGA and XRD analysis of compounds **1**–**6**, and XRD analysis of compound **7**, is available on the Web under http://www.sciencedirect.com or from the author.

CCDC-232390, -232391, -252101, and -249336 contain the supplementary crystallographic data in this paper for **2**, **3**, **4**, and **6**, respectively. These data can be obtained free of charge from The Cambridge Crystallographic Data Center via http://www.ccdc.cam.ac.uk/data_request/cif.

Appendix A. Supplementary material

Supplementary data associated with this article can be found in the online version at doi:10.1016/j.jssc.2008.11.018.

References

[1] S.R. Batten, R. Robson, Angew. Chem. Int. Ed. 37 (1998) 1461.
[2] N.W. Ockwig, O. Delgado-Friedrichs, M. O'Keeffe, O.M. Yaghi, Acc. Chem. Res. 38 (2005) 176.
[3] S. Kitagawa, R. Kitaura, S. Noro, Angew. Chem. Int. Ed. 43 (2004) 2334.
[4] J.L.C. Rowsell, E.C. Spencer, J. Eckert, J.A.K. Howard, O.M. Yaghi, Science 309 (2005) 1350.
[5] O.M. Yaghi, G.M. Li, H.L. Li, Nature 378 (1995) 703.
[6] M. Fujita, Y.J. Kwon, S. Washizu, K. Ogura, J. Am. Chem. Soc. 116 (1994) 1151.
[7] J.S. Seo, D. Whang, H. Lee, S.I. Jun, J. Oh, Y.J. Jeon, K. Kim, Nature 404 (2000) 982.
[8] L.-G. Qiu, A.-J. Xie, L.-D. Zhang, Adv. Mater. 17 (2005) 689.
[9] T. Sawaki, T. Dewa, Y. Aoyama, J. Am. Chem. Soc. 120 (1998) 8539.
[10] C.-D. Wu, W. Lin, Angew. Chem. Int. Ed. 46 (2007) 1075.
[11] R.Q. Zou, H. Sakurai, Q. Xu, Angew. Chem. Int. Ed. 45 (2006) 2542.
[12] D.N. Dybtsev, A.L. Nuzhdin, H. Chun, K.P. Bryliakov, E.P. Talsi, V.P. Fedin, K. Kim, Angew. Chem. Int. Ed. 45 (2006) 916.
[13] L. Alaerts, E. Seguin, H. Poelman, F. Thibault-Starzyk, P.A. Jacobs, D.E. De Vos, Chem. Eur. J. 12 (2006) 7353.
[14] C.D. Wu, A. Hu, L. Zhang, W.B. Lin, J. Am. Chem. Soc. 127 (2005) 8940.
[15] F.X.L.I. Xamena, A. Abad, A. Corma, H. Garcia, J. Catal. 250 (2007) 294.
[16] K.L. Wong, G.L. Law, Y.Y. Yang, W.T. Wong, Adv. Mater. 18 (2006) 1051.
[17] M. Alvaro, E. Carbonell, B. Ferrer, F.X.L.I. Xamena, H. Garcia, Chem. Eur. J. 13 (2007) 5106.
[18] F.X.L.I. Xamena, A. Corma, H. Garcia, J. Phys. Chem. C 111 (2007) 80.
[19] G.J. Halder, C.J. Kepert, B. Moubaraki, K.S. Murray, J.D. Cashion, Science 298 (2002) 1762.
[20] X.B. Zhao, B. Xiao, A.J. Fletcher, K.M. Thomas, D. Bradshaw, M.J. Rosseinsky, Science 306 (2004) 1012.
[21] M. Eddaoudi, J. Kim, N. Rosi, D. Vodak, J. Wachter, M. O'Keefe, O.M. Yaghi, Science 295 (2002) 469.
[22] B.L. Chen, N.W. Ockwig, A.R. Millward, D.S. Contreras, O.M. Yaghi, Angew. Chem. Int. Ed. 44 (2005) 4745.
[23] M.J. Zaworotko, Chem. Soc. Rev. 23 (1994) 283.
[24] B. Moulton, M.J. Zaworotko, Chem. Rev. 101 (2001) 1629.
[25] G.M. Sheldrick, SHELXS-97, Program for X-ray Crystal Structure Solution, University of Göttingen, Göttingen, Germany, 1997.
[26] G.M. Sheldrick, SHELXL-97, Program for X-ray Crystal Structure Refinement, University of Göttingen, Göttingen, Germany, 1997.
[27] A.L. Spek, PLATON, A Multipurpose Crystallographic Tool, Utrecht University, Utrecht, The Netherlands, 1999.
[28] S. Seelan, A.K. Sinha, Appl. Catal. A 238 (2003) 201.
[29] G. Bellussi, M.S. Rigutto, Stud. Surf. Sci. Catal. 85 (1994) 177.
[30] J.-M. Lehn, Supramolecular Chemistry—Concepts and Perspectives, Wiley-VCH, Weinheim, 1995, p. 4.
[31] J.M.S. Skakle, M.R.St.J. Foreman, M.J. Plater, Acta Crystallogr. E 57 (2001) m373.
[32] X.-M. Zhang, M.-L. Tong, M.-L. Gong, X.-M. Chen, Eur. J. Inorg. Chem. (2003) 138.
[33] M.J. Plater, M.R. St J. Foreman, R.A. Howie, J.M.S. Skakle, E. Coronado, C.J. Gómez-García, T. Gelbrich, M.B. Hursthouse, Inorg. Chim. Acta 319 (2001) 159.
[34] X. Shi, G. Zhu, Q. Fang, G. Wu, G. Tian, R. Wang, D. Zhang, M. Xue, S. Qiu, Eur. J. Inorg. Chem. (2004) 185.
[35] Y.-L. Fu, J.-L. Ren, S.W. Ng, Acta Crystallogr. E 60 (2004) m1716.
[36] X.-L. Wang, F.-C. Liu, J.-R. Li, S.W. Ng, Acta Crystallogr. E 61 (2005) m299.
[37] A. Bulut, H. Icbudak, O.Z. Yesilel, H. Ölmez, O. Büyükgüngör, Acta Crystallogr. E 59 (2003) m736.
[38] H.-P. Xiao, M.-L. Hu, X.-H. Li, Acta Crystallogr. E 60 (2004) m71.
[39] D.-Y. Wang, G. Liu, B. Zheng, H.-M. Hu, Acta Crystallogr. E 61 (2005) m925.